Phys Chem Minerals (2004) 31: 1–11
DOI 10.1007/s00269-003-0363-x

ORIGINAL PAPER

V. P. Solntsev · E. G. Tsvetkov · A. I. Alimpiev
R. I. Mashkovtsev

Valent state and coordination of cobalt Ions in beryl and chrysoberyl crystals

Received: 27 September 2002 / Accepted: 28 August 2003

Abstract We have studied the polarized optical absorption and EPR spectra of Co-doped beryls grown by hydrothermal, flux, and gas-transport methods, and chrysoberyl grown by the Czochralski method. In beryls three groups of bands, belonging to three various Co centers, were distinguished by analysis of the absorption band intensities. The first group, bands with maxima at 22 220 ($\mathbf{E} \perp \boldsymbol{c}$), 17 730 ($\mathbf{E} \parallel \boldsymbol{c}$), and 9090 ($\mathbf{E} \parallel \boldsymbol{c}$), 7520 ($\mathbf{E} \perp \boldsymbol{c}$) cm^{-1} are due to Co^{2+} in octahedral site of Al^{3+}. The second group is bands at 18 940, 18 250, 17 700 ($\mathbf{E} \perp \boldsymbol{c}$), 18 300, 17 700, 17 000 ($\mathbf{E} \parallel \boldsymbol{c}$) and 8830 ($\mathbf{E} \perp \boldsymbol{c}$), 7350 ($\mathbf{E} \parallel \boldsymbol{c}$) cm^{-1} and 5320 ($\mathbf{E} \perp \boldsymbol{c}$), 3880 ($\mathbf{E} \parallel \boldsymbol{c}$) cm^{-1}, which are caused by Co^{2+} in tetrahedral site of Be^{2+}. A weak wide band in flux and gas-transport beryl in the region of 12 500–8300 cm^{-1} ($\mathbf{E} \parallel, \perp \boldsymbol{c}$) is related to Co^{3+} in octahedral Al^{3+} site. In hydrothermal beryl, bands 13 200 ($\mathbf{E} \perp \boldsymbol{c}$), 10 900 ($\mathbf{E} \parallel \boldsymbol{c}$), and 8500 ($\mathbf{E} \perp \boldsymbol{c}$) cm^{-1} are caused by an uncontrolled impurity of Cu^{2+} ions. For Co-doped chrysoberyl one type of center of Co has been established: Co^{2+} in the octahedral site of Al^{3+}. In the approximation of the trigonal field with regard to Trees' correction, the energy levels of Co^{2+} have been calculated in octahedral and tetrahedral coordination. There is good agreement between the obtained experimental and calculated data. The polarization dependence of the optical absorption bands is explained well in terms of the spin-orbit interaction.

Keywords Beryl · Chrysoberyl · Optical absorption · EPR · Cobalt

V. P. Solntsev · E. G. Tsvetkov · A. I. Alimpiev
R. I. Mashkovtsev (✉)
Institute of Mineralogy and Petrography,
Novosibirsk 630090, Russia
e-mails: rim@uiggm.nsc.ru; tsvetkov@online.sinor.ru

Introduction

It is known that ions Ni and Co can occupy both octahedral and tetrahedral sites in beryl and chrysoberyl structures (Solntsev 1981). In this work the valency and coordination of Co ions in these structures are studied using EPR and optical absorption spectroscopy.

Beryl crystallizes in a hexagonal space group $P6/mcc = D^2_{6h}$ (Morosin 1972). The structure is sixfold rings $[Si_6O_{18}]$ consisting of SiO_4 tetrahedra connected with each other by BeO_4 tetrahedra and AlO_6 octahedra. The point symmetry of Si, Be, and Al sites is C_s, D_2, and D_3, respectively.

In chrysoberyl structure (space group $Pnma = D_{2h}{}^{16}$) there are two types of the oxygen octahedron in which Al^{3+} ions occupy sites with symmetry C_i and C_s, whereas Be^{2+} ions (point symmetry C_s) occupy tetrahedral sites (Farrell et al. 1963). Valence state and coordination of Co ions in hydrothermal synthetic beryl have been discussed in some works (Solntsev 1981; Evdokimova et al. 1989; Taran and Rossman 2001). The available interpretations of the optical spectra, EPR spectra, and data of X-ray diffraction experiment suggest several sites for Co^{2+} and Co^{3+} in the structure and different explanations for the optical absorption bands.

Sontsev (1981) proposed that intense bands at 22 200 ($\mathbf{E} \perp \boldsymbol{c}$), 17 730 ($\mathbf{E} \parallel \boldsymbol{c}$) cm^{-1}, and at 9090 ($\mathbf{E} \parallel \boldsymbol{c}$), and 7520 ($\mathbf{E} \perp \boldsymbol{c}$) cm^{-1} were due to Co^{2+} substituting for the Al^{3+} ion in the octahedral site: transitions $^4T_{1g}(^4E) \rightarrow {}^4T_{1g}(^4A_2, {}^4E)$ and $^4T_{1g}(^4E) \rightarrow {}^4T_{2g}(^4A_1, {}^4E)$, respectively. Weak bands at 18 940, 18 250, 17 700 ($\mathbf{E} \perp \boldsymbol{c}$), 18 300, 17 700, 17 000 ($\mathbf{E} \parallel \boldsymbol{c}$) cm^{-1}, and 8830 ($\mathbf{E} \perp \boldsymbol{c}$), 7350 ($\mathbf{E} \parallel \boldsymbol{c}$) cm^{-1} and 5320 ($\mathbf{E} \perp \boldsymbol{c}$), 3880 ($\mathbf{E} \parallel \boldsymbol{c}$) cm^{-1} were related to Co^{2+}, which occupy the Be tetrahedral site: transitions $^4A_2(^4A) \rightarrow {}^4T_1(^4B_2, {}^4B_3, {}^4B_1)$ and $^4A_2(^4A) \rightarrow {}^4T_1(^4B_2, {}^4B_3, {}^4B_1)$ and $^4A_2(^4A) \rightarrow {}^4T_2(^4B_2, {}^4B_3, {}^4B_1)$, respectively. The Co^{3+} ions in the octahedral site were responsible for the weak broad absorption band in the region 12 500–8300 cm^{-1} ($\mathbf{E} \parallel, \perp \boldsymbol{c}$). Taran and Rossman (2001) also assigned

intense bands at 22 300 ($\mathbf{E} \perp \boldsymbol{c}$), 17 800 ($\mathbf{E} \parallel \boldsymbol{c}$) cm^{-1}, and at 8700 ($\mathbf{E} \parallel \boldsymbol{c}$), 7400 ($\mathbf{E} \perp \boldsymbol{c}$) cm^{-1} as $^4T_{1g} \rightarrow {}^4T_{1g}$ (P) and $^4T_{1g} \rightarrow {}^4T_{2g}$ transitions, respectively, to Co^{2+} in the octahedral site. They noted that polarization properties and number of spin-allowed *dd* bands in the beryl spectrum were inconsistent with the assignment of either a $^4A_2$ or ^4E ground state of Co^{2+} originating from the split $^4T_{1g}$ level (Taran and Rossman 2001). Evdokimova et al. (1989), however, reported that in hydrothermal synthetic beryl Co^{2+} enters the Al octahedron [$^4T_{1g} \rightarrow {}^4T_{1g}$ (P) at 18 400 cm^{-1} and $^4T_{1g} \rightarrow {}^4T_{2g}$ at 8620 cm^{-1}], whereas Co^{3+} occupies both Be tetrahedral (7350 cm^{-1}) and Al octahedral sites (22 320 and 13 600 cm^{-1}).

Difficulties in reading the optical absorption spectra of Co-bearing hydrothermal synthetic beryl are due to the superposition of additional absorption bands from Cu^{2+} and Fe^{2+} ions in the region 14 000–7000 cm^{-1} and to vibronic coupling near 8500 and 5500 cm^{-1}. In order to avoid the influence of additional absorption bands, we have specially studied Co-doped flux-grown and gas-transport-grown beryls and two hydrothermal beryls with different contents of CuO (0.16 and 0.06 wt%). Beryl and chrysoberyl were studied for comparison, because in both crystals Co ions can enter octahedral and tetrahedral sites. To substantiate the correct assignment of the observed absorption bands and their polarization, we have calculated the parameters of crystal field of the Co^{2+} ions in octahedral and tetrahedral sites.

Experimental

Three types of Co-bearing synthetic beryl were studied:

1. Beryl crystals in hydrothermal fluoride and chloride solutions were grown at 600—650 °C in temperature gradient conditions. For this purpose we used steel autoclaves and proper oxides as major and trace components (Lebedev et al. 1988);
2. Beryl crystals were grown by a flux method in platinum containers at 1100—1150 °C under conditions of a reverse temperature gradient. We used appropriate oxides as major and trace components as well as mixtures $PbO–V_2O_5$ as solvent flux (Khranenko and Solntsev 1988);
3. The growth of beryl crystals was also conducted under gas-transport conditions in quartz ampoles at 1050—1100 °C. We used mixtures of different proportions of natural quartz, synthetic corundum, and ceramic BeO with minor cobalt oxides as starting components (Rodionov et al. 1987).

Chrysoberyl crystals with a small amount of cobalt were grown from stoichiometric melt with addition of the appropriate content of oxides at ~1970 °C. We used the Czochralski method, iridium crucibles, and argon protective atmosphere (Bukin et al. 1981).

The samples for investigation (Table 1) were prepared as oriented transparent self-supporting platelets polished on both sides. The initial orientation of samples was performed using well-developed faces ($10\bar{1}0$) (beryl), and (010); and (001) (chrysoberyl). The absorption spectra of the samples of beryl ($10 \times 10 \times 0.3$–0.5 mm) and chrysoberyl ($6 \times 5 \times 4$ mm) in the range of 30 000–4000 cm^{-1} were recorded on an SF-20 (LOMO, Leningrad) and Shimadzu 3100 spectrophotometers in polarized light at 300 K. The infrared absorption spectra in the range 4500–2500 cm^{-1} were recorded using a Brucker IFS 113v Fourier transform infrared spectrometer. The EPR spectra of Co-bearing beryl were measured at 4 K and frequency 74.51 GHz, using a spectrometer designed and built in the Donetsk Institute for Physics and Technology. The EPR spectra of chrysoberyl were recorded at frequency 9.3 GHz and temperatures 300 and 77 K, using a spectrometer RE-1306 designed and built in Novosibirsk (Institute of Chemical Kinetics). The grown beryl and chrysoberyl were analyzed for stoichiometry of composition, using spectrophotometry and the titration method for SiO_2 and Al_2O_3, respectively, and the atomic absorption method supplied with the Perkin-Elmer-400 technique for BeO and microimpurities. Trace oxide contents in crystals were detected by an X-ray microprobe method with a MS-46 Cameca analyzer (France), with an accuracy ~0.05 wt%. Results of analyses are given in Table 1.

Results

Electron paramagnetic resonance spectra

The EPR spectrum of the Co-doped flux-grown beryl at frequency 74.51 GHz and 4 K ($\mathbf{H} \parallel \boldsymbol{c}$) consists of sharp lines from Cr^{3+} and Fe^{3+} ions (uncontrolled impurities) and two additional wide lines with weakly resolved hyperfine structure from nuclear spin ^{59}Co ($I = 7/2$, 100% abundant) identified with two different Co^{2+} centers (Fig. 1). In addition to identified spectra, we observed two weaker lines near 1.35 and 3.92 T, whose nature was not established.

The first Co^{2+} center has an axial symmetry (single paramagnetic species in the unit cell, $K_m = 1$) and was described by spin-Hamiltonian with effective spin $S = 1/2$:

Table 1 Chemical composition of the studied crystals (wt%). *nd* = not detected

Sample	Oxides											
	SiO_2	Al_2O_3	BeO	CoO	Cr_2O_3	Fe_2O_3	CuO	Li_2O	Na_2O	K_2O	H_2O	Σ
Hydrothermal beryl A-146	66.11	18.86	13.84	0.98	nd	0.20	0.06	0.08	0.03	0.02	1.2	101.4
Hydrothermal beryl A-134	66.08	18.55	13.90	0.40	nd	0.17	0.16	0.04	0.10	nd	0.9	100.3
Flux beryl	66.61	18.72	13.86	1.02	0.03	0.02	nd	nd	nd	nd	nd	100.3
Gas-transport beryl	66.47	19.04	13.81	1.03	nd	nd	nd	nd	nd	nd	nd	100.4
Chrysoberyl	nd	78.80	20.70	0.02	nd	nd	nd	nd	nd	nd	nd	99.5

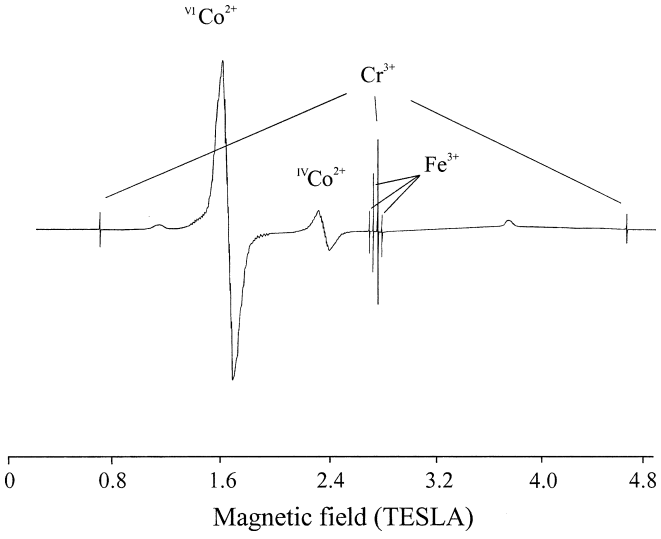

Fig. 1 EPR spectrum of Co-doped flux-grown beryl with magnetic field along the *c*-axis and at a frequency of 74.5 GHz and temperature of 4 K

$$H = \beta \boldsymbol{SgH} + \boldsymbol{IAS} \ ,$$

where β is the Bohr magneton, $\boldsymbol{H}$ is the magnetic field, $\boldsymbol{S}$ and $\boldsymbol{I}$ are the electron and nuclear spin operators, and $\boldsymbol{g}$ and $\boldsymbol{A}$ are tensors of spectroscopic spliting and hyperfine structure, respectively. The directions of the $\boldsymbol{g}_{\|}$ and $\boldsymbol{A}_{\|}$ center coincided with the Z axis of AlO_6 polyhedron ($Z \parallel \boldsymbol{c} \parallel [0001]$). Parameters of the center are as follows: $g_{\|} = 3.026$, $g_{\perp} = 4.758$, $A_{\|} = 3.5$ mT, $A = 8.6$ mT. The observed spectrum is assigned to Co^{2+} ion occupying the octahedral Al^{3+} site in the beryl structure. The Co^{2+} spectrum ($\boldsymbol{H} \parallel \boldsymbol{c}$) in beryl is represented by a poorly resolved line due to hyperfine structure with $A_{\|} = 3.5$ mT, on both sides of which we observed additional weak lines separated at $A_c \sim 9$–10 mT distance. These additional lines changed the shape of the main line, depending on the orientation of the magnetic field. We assume that the intricate structure of the spectrum is a result of the superposition of lines from exchange-coupled pairs of Co^{2+} on the main line. This phenomenon is expected because of the high concentration of Co ions (CoO $\sim$ 1 wt%, Table 1). In beryl, the spectra of exchange-coupled pairs of ions (Cr^{3+} −0.3 wt%, Ti^{3+} −0.25 wt%, and Fe^{3+} −0.3–0.5 wt%) have been studied in detail (Edgar and Hutton 1978, 1982; Kharchenko and Solntsev 1981a,b). It was shown that for spin S = 3/2 (Cr^{3+}, Co^{2+}) the most probable are 4th and 5th nearest-neighbour pairs wherein the ions are positioned at intervals of 9.193 and 9.212 Å along the crystal *c* axis and *a* axis, respectively. The spectra from these exchange-coupled pairs seem to contribute most significantly to the distortion of the main line from isolated Co^{2+} ion. We observed that the hyperfine splitting of exchange-coupled pairs was ~10 mT, whereas that of the main transition is 3.5 mT. Evdokimova et al. (1989) explained the intricate structure of Co^{2+} spectrum at $\boldsymbol{H} \perp \boldsymbol{c}$ by the presence of two inequivalent magnetic species ($K_m = 2$) in the unit cell. This statement appears to be erroneous, because for D_3 symmetry center (Al site) and spin S = 3/2 (Co^{2+}) one magnetic complex ($K_m = 1$) is expected (Rae 1969).

It is worth noting that after a γ-irradiation (Co^{60}, 5–100 Mrad, 77 K) in crystals of beryl (CoO $\sim$ 0.1 wt%) at 77 K we observed two additional EPR centers: O^--hole on oxygen of SiO_4 tetrahedron at which $Si^{4+} \leftarrow Al^{3+}$ [$g_c = 2.014$, $^{27}A_c(Al) = 0.7$, $^{9}A_c(Be) = 0.2$ mT], and $Al^{2+} \rightarrow Be^{2+}$ [$g_c = 1.9962$, $^{27}A_c = 39.1$ mT], which were described earlier (Solntsev and Khranenko, 1989).

The second Co^{2+} center ($g_x = g_c = 2.231$) is described by the effective spin S = 1/2 and has three inequivalent magnetic complexes in the unit cell ($K_m = 3$), with axes Z, Y, and X coinciding with $[2\bar{1}\bar{1}0]$, $[01\bar{1}0]$, and [0001], respectively. The spectrum of the second center is also represented by a wide line with a poorly resolved hyperfine structure similar to Co^{2+} in Al octahedron. Unfortunately, because of the overlapping of the spectra of three complexes and the exchange-coupled pairs of ions, we failed to measure the *g* and *A* factors accurately. Approximate parameters were $g_x = 2.231 \pm 0.008$, $A_x = 8$ mT, $g_y = 2.09 \pm 0.08$, $A_y = 9$ mT, $g_z = 3.27 \pm 0.05$, $A_z = 25$ mT. The observed symmetry of Co^{2+} is consistent only with the site of Be^{2+}. The spectrum intensity of octahedral $^{VI}Co^{2+}$ at $\boldsymbol{H} \parallel \boldsymbol{c}$ is 5–7 times greater than that of tetrahedral $^{IV}Co^{2+}$.

Analysis of *g* and *A* parameters of ions $^{VI}Co^{2+}$ and $^{IV}Co^{2+}$ in beryl has shown that it is difficult to explain them only by the ground state d_{z^2} or $d_{x^2-y^2}$ ($^{VI}Co^{2+}$) or d_{xy} ($^{IV}Co^{2+}$). In distorted octahedral low-spin Co^{2+} complexes Maki et al. (1964) gave the following equations taking spin-orbit coupling into consideration. For $(d_{x^2-y^2})^2(d_{z^2})^1$ configuration: $\boldsymbol{g}_{\|} = 2.0$, $\boldsymbol{g}_{\perp} = 2 - 6a_1$, where $a_1 = \zeta/\Delta(z^2 - xz, yz)$. For $(d_{z^2})^2(d_{x^2-y^2})^1$ configuration: $\boldsymbol{g}_{\|} = 2 - 8b_1$, $\boldsymbol{g}_{\perp} = 2 - 2b_2$, where $b_1 = \zeta/\Delta(\{x^2 - y^2\} - xy)$, $b_2 = \zeta/\Delta(\{x^2 - y^2\} - xz)$, where $\zeta = -540\,\mathrm{cm}^{-1}$ is the one-electron spin-orbit coupling constant of Co^{2+}, and $\Delta(z^2{-}xz)$, etc. represent the energy separation between $(d_{x^2-y^2})^2(d_{z^2})^1$ and $(d_{x^2-y^2})^2(d_{xz})^1$, etc. The obtained equations do not explain experimental data. If we consider mixing only of d_{z^2} and $d_{x^2-y^2}$, the orbital wave function of the ground state can be written as $\Psi_{z^2} = \alpha d_{z^2} + \beta d_{x^2-y^2}$. Assuming *d*-orbital pure and using the theory perturbation in the first and second order, McGarvey (1969) has written the following equations for spin-Hamiltonian parameters: $\boldsymbol{g}_{\|} = 2 - 8\beta^2\zeta/\Delta E_{xy}$, $\boldsymbol{g}_{\perp} = 2 - 2\zeta(3\alpha^2 + \beta^2)/\Delta E_{xz,yz}$; $\boldsymbol{A}_{\|} = \mathrm{P}\{-\alpha^2\mathbf{k} + 4/7(\alpha^2 - \beta^2) + 6\zeta(\alpha^2 - \beta^2)/7\Delta E_{xz} - 8\zeta\beta^2/\Delta E_{xy}\}$, $\boldsymbol{A}_{\perp} = \mathrm{P}\{-\alpha^2\mathbf{k} - 2/7 (\alpha^2 - \beta^2) - 3\zeta(\alpha^2 - \beta^2)/7\Delta E_{xz} - 2\zeta(3\alpha^2 + \beta^2)/\Delta E_{xz}\}$. $\mathbf{k}$ is a parameter referring to the Fermi hyperfine coupling energy in units $P = 2\beta g_n \beta_n r^{-3}$. These equations allow explanation of experimental data only qualitatively. When analyzing experimental data of Co^{2+} in Al_2O_3 [$\boldsymbol{g}_{\|} = 2.292$, $\boldsymbol{g}_{\perp} = 4.947$, $\boldsymbol{A}_{\|} = 3.24\,\mathrm{mT}$, $\boldsymbol{A}_{\perp} = 9.72\,\mathrm{mT}$ (Zverev and Prokhorov 1960)], Ray (1961) showed that for precise quantitative calculation of parameters EPR it is necessary to take into account mixing of d_{z^2} and $d_{x^2-y^2}$ and

other excited configurations as well as covalence. As in D_3-trigonal distorted octahedral CoO_6 complexes d_{z^2}, $d_{x^2-y^2}$, d_{xz}, d_{yz} and p_x, p_y orbitals have E symmetry, they can be mixed.

The EPR analysis of Co-doped chrysoberyl has shown that here, as in beryl at 77 and 300 K, no spectra from Co ions are observed. However, after an γ-irradiation, EPR signal from 16 equidistant lines with an approximate ratio 1:3:6:10:15:21:25:27:27:25: ...:3:1 was observed. The center is identified with hole(O^-) of one oxygen of BeO_4 tetrahedron in which Be is replaced by Al. This hole cooperates poorly with three ^{27}Al [$g_c = 2.074$, $A_c(Al_1) = 0.67$, $A_c(Al_2,\ Al_3) = 0.56$ mT, $g_c \sim$ along short-bond Be–O = 1.579 Å]. The data obtained suggest that the charge of Co^{2+} lacking in octahedral sites in beryl and chrysoberyl is compensated for by the occurrence of Al^{3+} in the site of Be^{2+}. As the EPR spectra from ions Co are not observed, further study of the valent state and coordination of Co ions in chrysoberyl is based on optical absorption spectra and their comparison with the corresponding spectra in beryl.

Optical absorption spectra

The difficulty in determining the coordination of Co ions from the optical spectra arises from the fact that the absorption bands of Co ions in octahedral [17 730(π), 9090(π) and 7520(σ)] and tetrahedral sites [18 940–17 700($\sigma+\pi$), 8830(σ), and 7350(π)] are localized in the same spectral regions of the spectra. The absorption spectrum of Co-doped flux beryl in polarized light (Fig. 2a,b) consists of several broad absorption bands in the range 27 000–3500 cm^{-1}, complicated by additional narrow bands. Analysis of absorption bands in flux, hydrothermal, and gas-transport-grown beryls as well as

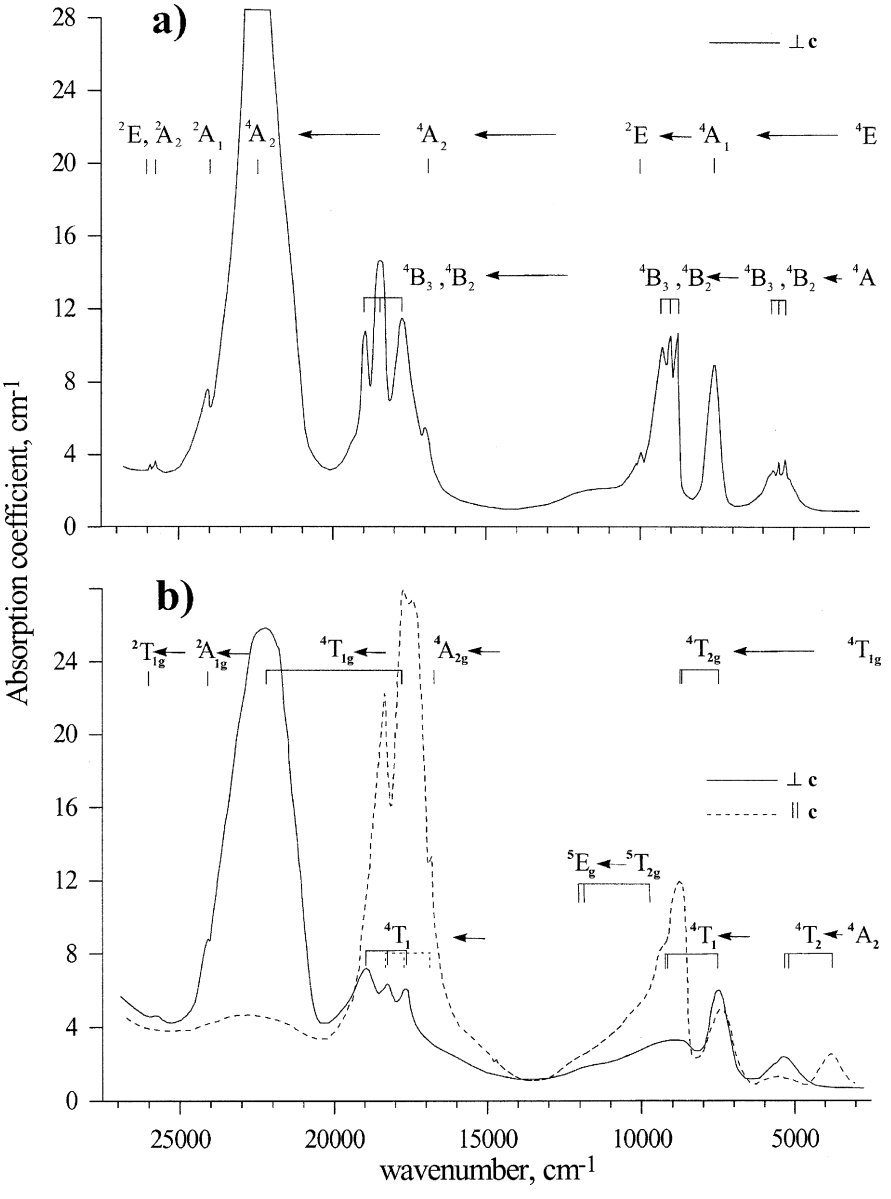

Fig. 2a–c Polarized electronic absorption spectra of Co-doped flux-grown beryl at (**a**) 80 K (**E** ⊥ ***c***) and (**b**) 300 K. (**c**) Polarized electronic absorption spectra of Co + Cu-doped hydrothermal beryl at 300 K. In the *upper part of the figure* the position of energy levels $^{VI}Co^{2+}$ is shown, whereas the position of energy level $^{IV}Co^{2+}$ is *lower*, at **E** ⊥ ***c***

Fig. 2a–c (Contd.)

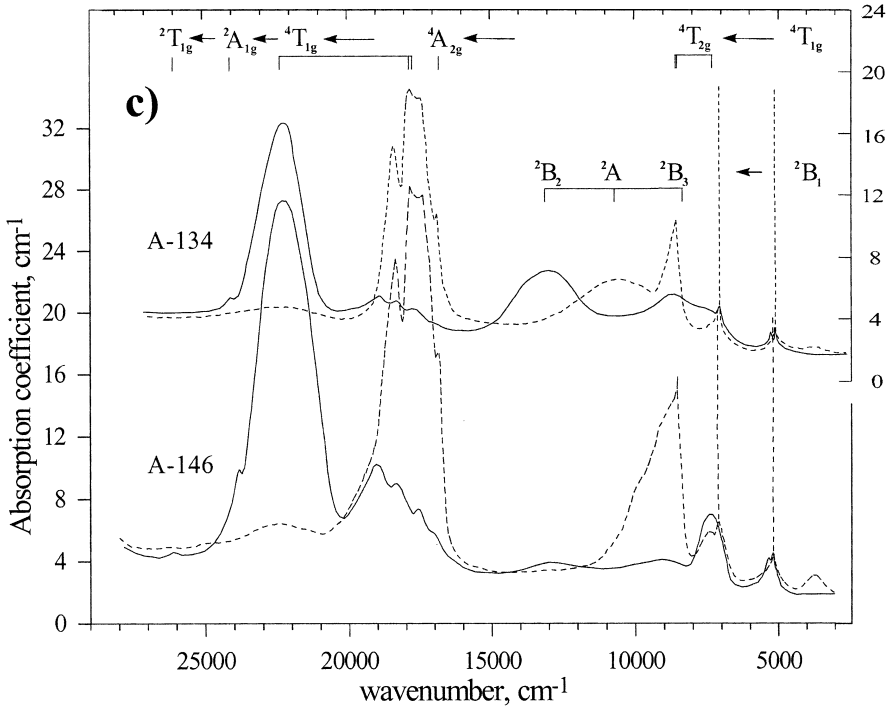

EPR data point to the presence of three different Co centers. Analysis of the optical absorption and EPR spectra has allowed us to identify the band with maxima at 22 220 (σ), 17 730 (π), 9090(π), and 7520(σ) cm^{-1} with *dd* transition of Co^{2+} in the octahedral position of Al^{3+}. The assignment of intense bands 22 300(σ), 17 800(π), 8700(π), and 7400(σ) cm^{-1} to Co^{2+} in the Al octahedron was discussed in detail by Taran and Rossman (2001). A similar spectrum from Co^{2+} ions in octahedron with trigonal distortion (C_{3v}), consisting of two broad bands in the region 21 500–18 650 and 11 000–8500 was also observed in corundum (Townsend 1964).

The bands with maxima at 18 940, 18 250, 17 700(σ), 18 300, 17 700, 17 000(π) cm^{-1} and 8830(σ), 7350(π) and 5320(σ), 3880(π) cm^{-1} and narrow bands we identified with Co^{2+} in tetrahedral site of Be^{2+}. The fact that Co^{2+} replaces Be^{2+} in beryl (except Al^{3+}) was proved by the observation of EPR spectrum of Co^{2+} and additional bands of optical absorption, which were not described by Evdokimova et al. (1989) or Taran and Rossman (2001). These bands 5320(σ) and 3880(π) cm^{-1} are $^4A_2(F)[^4A] \rightarrow {}^4T_2(F)[^4B_3, {}^4B_2, {}^4B_1]$ transitions of Co^{2+} in the Be tetrahedron ($^{IV}Co^{2+}$). Other transitions originating from $^4A_2(F) \rightarrow {}^4T_1(F)$ and $^4A_2(F) \rightarrow {}^4T_1(P)$ fall into the absorption region of the octahedral Co^{2+} ions ($^{VI}Co^{2+}$). However, comparison of the intensities of bands 3880 cm^{-1} and 5320 cm^{-1} with the intensity of sharp lines 18 300(π) and 17 700(σ), 18 250(σ), and 18 940(σ) cm^{-1} shows that they have a constant ratio in the flux-grown and gas-transport-grown beryls and, hence, are related to the same Co^{2+} center in the Be tetrahedron. When the temperature decreased to 80 K, in the spectrum of Co-containing flux beryl one could clearly see a triplet splitting (Fig. 2a), which allowed the position of maxima of absorption bands of $^{IV}Co^{2+}$ to be determined. The $^4A_2(F) \rightarrow {}^4T_1(P)$, $^4T_1(F)$, $^4T_2(F)$ transition is split into a triplet, which is typical of cobalt in tetrahedral coordination (Akridge and Kennedy 1979). The orientations of axes of the optical indicatrix (*X*, *Y*, *Z*) against the crystallographic axes in beryl were as follows: for $AlO_6(CoO_6)$ octahedron $Z \parallel [0001] \parallel \boldsymbol{c}$, X, $Y \perp \boldsymbol{c}$ and $BeO_4(CoO_4)$ tetrahedron – $Z \parallel [2\bar{1}\bar{1}0] \parallel \boldsymbol{a}$, $X \parallel \boldsymbol{c} \parallel [0001]$, $Y \parallel [01\bar{1}0] \perp \boldsymbol{a}$. It is worth noting that in the spectrum of hydrothermal beryl, the bands in the field 6000–10 000 cm^{-1}, interpreted usually as the $^4T_{1g}(F) \rightarrow {}^4T_{2g}(F)$ transition of Co^{2+} ion in octahedral coordination (Wildner and Langer 1994; Wildner 1996), are superimposed by strong, sharp absorption lines (Fig. 2c) caused by overtones and combination vibrations of H_2O molecules in structural channels (Wood and Nassau 1968). As expected, such absorptions are absent in the spectrum of the flux and gas-transport-grown beryls. Otherwise, the spectrum of flux and gas-transport-grown beryls is similar to that of hydrothermal beryl. The only noticeable difference is that the bands at 13 300(σ) cm^{-1}, 10 900(π), and 8500(σ) cm^{-1} are absent in the flux-grown and gas-transport-grown beryls. These absorption bands in hydrothermal beryls were expected, as the samples contained appreciable amount of Cu^{2+} ions in the Be tetrahedron (see Table 1, Fig. 2c; Solntsev 1981; Solntsev et al. 1976).

In a regular tetrahedron of T_d symmetry the ^2D term of the Cu^{2+} ion split into doublet (E) and triplet (T_2). In tetragonally D_{2d} distorted tetrahedron, the perturbation parameter is given by the angle β between the Z axis of complex and the Cu-ligand vector. According to the deformation angle, we have a regular tetrahedron ($\beta = 54.74°$). When the tetrahedron undergoes elongation

($\beta = 0°\div45°$), the ground state is d_{z^2}. In the compressed tetrahedron, d_{xy} is the ground state if $\beta = 54.74$–$90°$ (Hofmann and Goslar 1982). Axes Z, Y, X of the Cu^{2+} center in beryl, from the EPR data (Solntsev et al. 1976), coincided with $[2\bar{1}\bar{1}0] \parallel \boldsymbol{a}$, $[01\bar{1}0] \perp \boldsymbol{a}$, and $[0001] \parallel \boldsymbol{c}$ crystals, respectively. According to the rules of selection for D_2 symmetry with such installation (Table 2) for ion Cu^{2+}, transitions $^2B_1 \rightarrow {}^2B_2 = 13\ 300(\sigma)$, $^2B_1 \rightarrow {}^2B_3(\sigma) = 8500$, and $^2B_1 \rightarrow {}^2A = 10\ 900(\pi)$ cm^{-1} were observed (Fig. 2c).

Finally, a weak broad band in the region 12 500–8300(π) cm^{-1} is assigned to Co^{3+} ions in the octahedral site of Al^{3+} (Fig. 2a,b). For Co^{3+} ion in the Al octahedron two alternatives of the ground state are possible: $^5T_2$ (at $Dq < 2B$ and $C = 4.808$ B) or $^1A_1(t_2^6)$ at $Dq > 2B$. In the former case, one observes two broad overlapped bands with close maxima. In the latter case, there are two broad bands in the visible and near-UV range, for example, Co^{3+} in Al_2O_3–15 500 cm^{-1} and 23 000 cm^{-1} (McClure 1962). Usually Dq for Cr^{3+}, Ti^{3+}, and Mn^{3+} ions in beryl is 1.11–1.14 times less than Dq of these ions in Al_2O_3. This is expected, as the ratio Dq in corundum ($R_{Al–O} = 1.856$ Å) to Dq in beryl ($R_{Al–O} = 1.904$ Å) for particular ions is in inverse proportion to ratio R^5 and equals 1.136. Taking this into account, two wide absorption bands near 14 000 and 20 800 cm^{-1} would have been expected for Co^{3+} in beryl, if $^1A_1$ had been the ground state. If, as Evdokimova et al. (1989) assumed, octahedral Co^{3+} is also present in beryls, it undoubtedly constitutes only a very small part of total Co content. The absorption bands arising from $^1A_{1g} \rightarrow {}^1T_{2g}$ transitions should be observed close to 14 000 and 20 800 cm^{-1}. As in flux-grown and gas-transport-grown beryl no bands were observed in the 13 000–15 000 cm^{-1} range, a weak broad band in the range 12 500–8300 cm^{-1} is most likely related to Co^{3+} ions with $^5T_2$ ground state ($^5T_2 \rightarrow {}^5E$). The scheme of splitting of energy levels Co^{3+} in Al octahedron of beryl is shown in Fig. 6.

Analysis of the lasing and optical properties of $BeAl_2O_4$: Cr^{3+}, Ti^{3+}(Bukin et al. 1978, 1981; Walling et al. 1980; Shand and Walling 1982; Alimpiev et al. 1986) and the EPR spectra of Cr^{3+}, Ti^{3+}, Mn^{2+}, and Fe^{3+} ions (Barry and Troup 1969, 1970; Solntsev 1981, 1982; Forbes 1983) has shown that they replace in chrysoberyl structure two physically distinct octahedral sites Al^{3+}: a mirror site (C_s)–(Al-O)$_{aver.}$ = 1.934 Å and inversion site (C_s)–(Al-O)$_{aver.}$ = 1.890 Å. These researches have shown that approximately three quarters of the transition metal atoms occupy a mirror site. In general, if the ion site posesses inversion symmetry, parity forbids electric dipole transitions between states of the d^7 configuration. As a consequence, a Co^{2+} ion that resides on an inversion site will have a weak magnetic-dipole no-phonon and phonon transitions as a Cr^{3+} (Walling et al. 1980). Therefore, here we shall discuss only Co^{2+} in a mirror site.

The absorption spectrum of Co-doped chrysoberyl (Fig. 3) is represented by broad anisotropic bands of absorption in the ranges 22 000–17 000 and 10 000–7000 cm^{-1}, and by weaker narrow bands with maxima close to 15 000 and 6500 cm^{-1}. The intense spectrum from broad bands was similar to a spectrum Co^{2+} in corundum (Townsend 1964) and is identified with Co^{2+} in the octahedral site $Al^{3+}(C_s)$ $BeAl_2O_4$. In octahedral symmetry Co^{2+} has a ground state $^4T_{1g}(F)$ and the lowest d–d excited states are: $^4T_{2g}(F)$, $^4A_{2g}(F)$ and $^4T_{1g}(P)$. Clearly, in O_h symmetry there are only three spin-allowed transitions, i.e., those of quartet states $^4T_{2g}(F)$, $^4A_{2g}(F)$, $^4T_{1g}(P)$. Under the perturbation $O_h \rightarrow D_{3d} \rightarrow D_3$ (beryl) or $O_h \rightarrow D_{3d} \rightarrow C_s$ (chrysoberyl) the degeneracies of these states are removed, as represented in Fig. 4. Note that the ground state in chrysoberyl splits into three states, i.e., $^4T_{1g}(F) \rightarrow {}^4A'' + {}^4A' + {}^4A''$, and the lowest is the new ground state ($^4A''$). The transitions $^4A'' \rightarrow {}^4A'$ are allowed in Z polarization, and $^4A'' \rightarrow {}^4A''$ in X and Y polarization (Table 2). Orientation of axes of the optical indricatrix (X, Y, Z) against the crystallographic axes for octahedral site (C_s) in chrysoberyl was as follows: axis Y coincided with axis $\boldsymbol{b}$ of the crystal, Z axis deviated from the axis $\boldsymbol{c}$ by 3.63° in plane $\boldsymbol{ac}$, and the axis X lies in plane $\boldsymbol{ac}$ at an angle of 93.63° from axis $\boldsymbol{c}$. The symmetry of AlO_6 octahedron is close to trigonal (C_3), if minor contributions of fields of lower symmetry are neglected.

The symmetry of the BeO_4 tetrahedron in chrysoberyl can be treated also as close to C_3, if minor contributions of fields of lower symmetry are neglected. Thus, the axis Y is parallel to the direction O_3–O_3 of tetrahedgon, and the Z axis coincides with the direction of short-bond Be–O_1 (1.579 Å) and makes a 0.83° angle with axis $\boldsymbol{c}$. Comparison of $^{IV}Co^{2+}$ spectra in beryl with Co^{2+} spectra in chrysoberyl allows the bands in the ranges 16 000–15 380 and 7040–6130 cm^{-1} to be attributed to $^4A_2(F) \rightarrow {}^4T_1(P)$ and $^4T_1(F)$ to transitions Co^{2+} in the tetrahedral site $Be^{2+}(C_s)$ or $^4T_{1g}(F) \rightarrow {}^2T_{2g}(G)$, $^2T_{1g}(H)$ and $^2E_g(G)$ transitions Co^{2+} in octahedral site $Al^{3+}(C_s)$. As no

Table 2 Selection rules for electric dipole transitions in crystalline fields of symmetry D_3, D_2, and C_s. (Herzberg 1969)

D_3	A_1	A_2	E	$E_{1/2}$	$E_{3/2}$	D_2	A	B_1	B_2	B_3	$E_{1/2}$	C_s	A′	A″	$E'_{1/2}$
A_1	0	π	σ			A	0	x	y	z		A′	x,y	z	
A_2	π	0	σ			B_1	x	0	z	y		A″	z	x,y	
E	σ	σ	$\pi+\sigma$			B_2	y	z	0	x		$E'_{1/2}$			x,y,z
$E_{1/2}$				$\pi+\sigma$	σ	B_3	z	y	x	0					
$E_{3/2}$				σ	π	$E_{1/2}$					x,y,z				

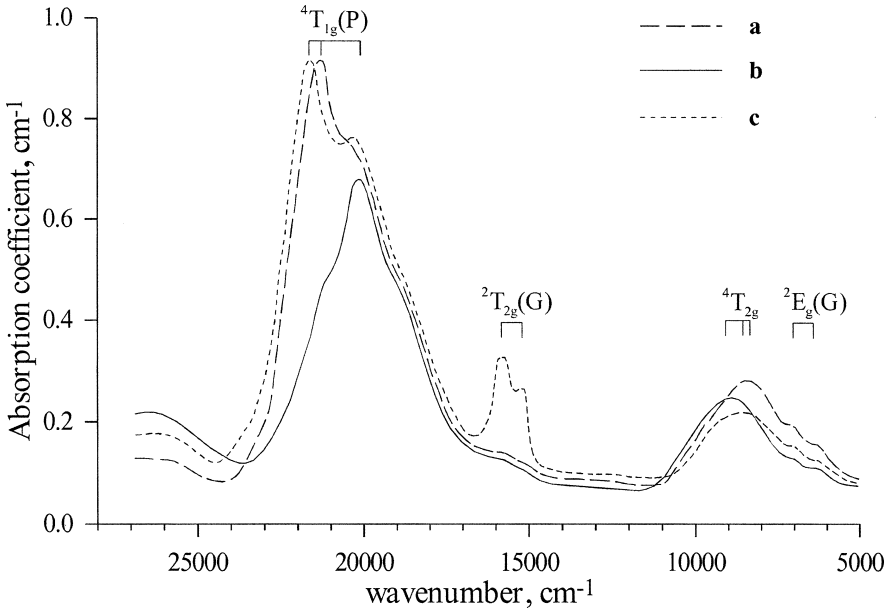

Fig. 3 Polarized electronic absorption spectra of Co-doped chrysoberyl at 300 K

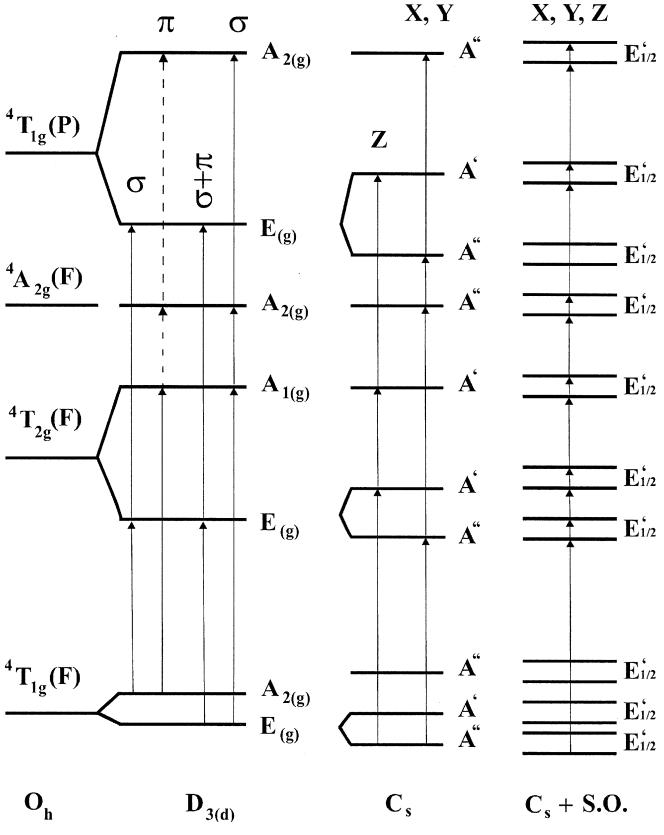

Fig. 4 Scheme of splitting of energy levels of Co^{2+} in octahedral sites at decreasing symmetry of enviroment $O_h \rightarrow D_{3d} \rightarrow D_3$ or $O_h \rightarrow D_{3d} \rightarrow C_s$. For D_3 symmetry index (g) should be omitted

bands in the region 5000–4000 cm^{-1} were revealed, weak bands close to15 380 and 7040 cm^{-1} most likely belong to $^4T_{1g}(Al) \rightarrow {}^2T_{2g}(A'',A',A')$, $^2T_{1g}(A'',A',A'')$ and $^2E_g(A'',A')$ transitions $^{VI}Co^{2+}$, respectively.

To process spectra, we made our computer calculations using the energy matrix of $d^3(d^7)$ electrons, considering $V_{cub} + V_{ee} + \alpha L(L + 1) + V_{trig}$ (Sviridov et al.1976; Veremeichik et al. 1977) in the strong cubic field approach. Term α takes into account interconfiguration or orbit–orbit interaction (Trees 1951,1952). As a first step in the analysis of the optical spectrum of Co^{2+} in $Be_3Al_2Si_6O_{18}$ and $BeAl_2O_4$, the appropriate electrostatic and crystal-field matrices were combined with trigonal crystal-field matrices.The combined interaction matrices were diagonalized for different values of the Racah *B, C,* octahedral crystal-field parameter $\Delta(=10Dq)$ and trigonal field parameters v, v'. The dependence of various bands on these parameters was then examined.

When searching for parameters characterizing the positions of levels in the cubic crystal field, the barycenter of absorption bands is generally assumed to be the same as in low-symmetry fields. Estimation of the shift of center of gravity showed that for $^{VI}Co^{2+}$ in beryl crystals the trigonal field decreases the energy of the states $^2E(G)$ and $^2T_1(G)$ and increases the energy of the $^2T_2(G)$ term by ~930, 537, and 213 cm^{-1}, respectively. For broad bands these values vary from ~100 to 430 cm^{-1}. To avoid a mistake caused by the shift of the barycenter, in determining parameters of cubic field the search for Dq, B, C, and α was conducted taking into account the components of terms at fixed v and v'.The shift of the barycenter owing to the fields of lower symmetry and spin-orbit interaction was neglected. The calculation of low-symmetry spectra of $^{VI}Co^{2+}$ in chrysoberyl was performed in a trigonal approach. For the mirror site in chrysoberyl the six oxygens can be considered to form two equilateral triangles centered on the ***c*** axis. In an undistorted octahedron the polar angle θ between a ligand direction and threefold

symmetry axis ***c*** is 54.75°. In chrysoberyl the octahedron is distorted. Polar angles for the upper triangle were 56.8, 56.8, and 53.0°, and for the lower triangle 54.5, 54.5, and 65.5°. As a result, the line passing through the barycenters of the upper and lower triangles and the Al atom (axis Z of the center) deviated from axis ***c*** by 3.63° in plane ***ac***. Such an arrangement of axes for the Cr^{3+} (C_s) center in chrysoberyl is established experimentally (Forbes 1983). Thus, the symmetry of the AlO_6 octahedron is close to trigonal (C_3), if minor contributions of fields of lower symmetry are neglected (Sviridov and Smirnov 1977). As was mentioned above, the symmetry of the BeO_4 tetrahedron in chrysoberyl can also be regarded as close to C_3. It is more difficalt to present pseudotrigonal distortion of BeO_4 polyhedron in beryl structure at $Co^{2+} \rightarrow Be^{2+}$ replacement. This required a significant distortion of BeO_4 tetrahedron. Therefore, calculation of the levels $^{IV}Co^{2+}$ in beryl is carried out in cubic (Table 4, footnote[a]) approximation. For an estimation of anisotropic parameters of spectra $^{IV}Co^{2+}$ calculation in trigonal approximation has been carried out (Table 4, footnote[b]). The splitting of the levels of Co^{2+} in octahedral and tetrahedral positions with different distortions are shown in Figs. 4 and 5. The selection rules for electric dipole transitions in Co^{2+} ions in crystalline fields of D_3, D_2, and C_s symmetry are given in Table 2. Calculated and experimental values for the energy of Co^{2+} terms in octahedral and tetrahedral sites are listed in Tables 3 and 4.

Discussion

As seen from Fig. 4, the $^4T_{1g}(F)$ term of Co^{2+} in octahedral site is split into ^4E and ^4A levels in the trigonal field (D_3) of beryl. At a certain ratio of parameters v and v' the degeneracy of $^4T_{1g}(F)$ term is not removed. So, at $Dq = 914$, $B = 820$, $C = 3880$, and $v = 2169$, $v' = -1901$, $\alpha = 110\ cm^{-1}$ the $^4T_{1g}(F)$ term is not split. Therefore, no matter whether ^4E or ^4A is the ground state, the position of the other levels of the term $^4T_{1g}(P)$ corresponds to $^4A_2 = 22\ 238$ and $^4E = 17\ 730$, while for the term $^4T_{2g}(F)$ it corresponds to $^4A_1 = 9090$ and $^4E = 7990\ cm^{-1}$, respectively. At minor splitting of the $^4T_{1g}(F)$ term the polarization dependence of Co^{2+} spectrum is determined by either ^4E or $^4A_2$ ground states. Thus, for the ground state the ^4E position of energy levels of $^{VI}Co^{2+}$ in beryl is well described by parameters $Dq = 914$, $B = 820$, $C = 3880$, $v = 2750$, $v' = -1810$, $\alpha = 120\ cm^{-1}$ (Table 3, footnote[a]). Whereas for the ground state $^4A_2$, the calculated values of energy levels $^{VI}Co^{2+}$ (Table 3, footnote[b]) are in much poorer agreement with experimental data and do not explain polarizing dependence. Consideration of spin-orbit coupling leads to the following splitting: $^4A_2 \rightarrow E_{1/2} + E_{3/2}$, $^2E \rightarrow E_{1/2} + E_{3/2}$, $^2T_1 \rightarrow 2E_{1/2} + E_{3/2}$, $^2T_2 \rightarrow 2E_{1/2} + E_{3/2}$, $^2A_1 \rightarrow E_{1/2}$, $^2A_2 \rightarrow E_{1/2}$, and $^4E \rightarrow 3E_{1/2} + E_{3/2}$. Calculation of this splitting in the approximation of cubic field in the first order leads to

Table 3 Calculated and experimental levels of Co^{2+} energy in octahedral sites of beryl and chrysoberyl

Beryl						Chrysoberyl			
Term	Level	Experiment	$\parallel c$	Calculation		Level	Experiment	$\parallel c$, $\parallel a$,	Calculation
(O_h)	(D_3)		$\perp c$	1[a]	2[b]	(C_s)		$\parallel b$	3[c]
	E			0	1737	A″			0
$^4T_{1g}$ (F)	A_2			653	0	A′			0
						A″			897
	E	7520	$\perp + \parallel$	7963	9527	A″	8150	$\parallel a, c$	8237
$^4T_{2g}$ (F)	A_1	9090	$\parallel + \perp$	9473	8280	A′	8330	$\parallel a, c$	8237
						A′	8930	$\parallel b, a$	9127
^2E_g (G)		8700	$\perp + \parallel$	8656	9828	A″ A′	8000	$\parallel a, c$	8162
$^4A_{2g}$ (F)		17 000	$\perp$	16 523	20 226	A″			17 794
	E			16 505	17 226	A″ A′			15 677
$^2T_{1g}$ (G)	A_2			16 411	16 105	A″			16 431
	E	17 730	$\parallel + \perp$	17 830	21 900	A′	20 080	$\parallel b$	19 894
							20 160	$\parallel a$	
$^4T_{1g}$ (P)	A_2	22 220	$\perp$	22 354	17 244	A″	20 240	$\parallel c$	19 894
							21 410	$\parallel b$	
						A″	21 550	$\parallel a$	21 589
							21 650	$\parallel c$	
	E			17 411	18 439	A″ A′			15 677
$^2T_{2g}$ (H)	A_1			15 731	18 784	A′			15 799
	E			21 647	21 854	A″ A′			20 658
$^2T_{1g}$ (H)	A_2			21 053	22 385	A″			20 294
$^2A_{1g}$ (G)		24 030	$\perp$	23 820	23 390	A′			23 000
	E	26 040	$\perp$	22 554	25 592	A″ A′			23 948
$^2T_{1g}$ (F)	A_2			27 006	28 478	A″			26 133

[a] $Dq = 914$, $B = 820$, $C = 3880$, $v = 2750$, $v' = -1810$, $\alpha = 120\ (cm^{-1})$
[b] $Dq = 914$, $B = 842$, $C = 3970$, $v = -2900$, $v' = 1045$, $\alpha = 0\ (cm^{-1})$
[c] $Dq = 940$, $B = 860$, $C = 3700$, $v = 1650$, $v' = -610$, $\alpha = 0\ (cm^{-1})$

Table 4 Calculated and experimental levels of Co^{2+} energy in tetrahedral sites of beryl

Term (T_d)	Level (D_2)	Experiment			Calculation	
		300 K	(**E** $\|\|\perp$ ***c***)	80 K (**E** $\perp$ ***c***)	1[a]	2[b]
$^4T_2(F)$	B_1	3880	$\| + \perp$	5500		4338
	B_2	5320	$\perp + \|$	5340		4974
	B_3	5320	$\perp + \|$	5210	4820	4974
$^4T_1(F)$	B_1	7350	$\| + \perp$	8570		7358
	B_2	8830	$\perp + \|$	8860		
	B_3	8830	$\perp + \|$	9050	8278	8808
$^4T_1(P)$	B_1	17 670	$\| + \perp$	17 800		17 507
	B_2	18 300	$\perp + \|$	18 300		18 320
	B_3	18 300	$\perp + \|$	19 150	18 031	18 320
$^2E(G)$					15 320	15 041
	B_1				15 860	15 957
$^2T_1(G)$	B_2, B_3					15 971
$^2A_1(G)$					18 330	18 273
	B_1				19 227	18 683
$^2T_2(G)$	B_2, B_3					19 080
	B_1				21 356	21 202
$^2T_2(H)$	B_2, B_3					21 054
	B_1				20 857	21 590
$^2T_1(H)$	B_2, B_3					21 400

[a] $Dq = 482$, $B = 790$, $C = 3450$, $v = 0$, $v' = 0$, $\alpha = 0$ (cm^{-1})
[b] $Dq = 482$, $B = 790$, $C = 3450$, $v = -1450$, $v' = -100$, $\alpha = 0$ (cm^{-1})

splitting of $^4T_{1g}$ (F), $^4T_{2g}$(F) and $^4T_{1g}$(P) terms into three levels (Pappalardo et al. 1961), each with shifts ($\zeta = -540$ cm^{-1}): $^4T_{1g}(F) = -633$, -253, $+380$ cm^{-1}, $^4T_{2g}(F) = -135$, $+90$, $+225$ cm^{-1}, $^4T_{1g}(P) = -245$, $+163$, $+408$ cm^{-1}. For the ground state $^4E_{1/2}$ transitions $E_{1/2} \rightarrow E_{1/2}$ are allowed in (π + σ)-, and $E_{1/2} \rightarrow E_{3/2}$ in σ-polarization; for the ground state $^4E_{3/2}$ transitions $E_{3/2} \rightarrow E_{1/2}$ in σ- and $E_{3/2} \rightarrow E_{3/2}$ are allowed in π-polarization. The EPR data show that the ground state of $^{VI}Co^{2+}$ in beryl represents a mix of d_{z^2} + $d_{x^2-y^2}$ and other excited states and, hence, there is a probability of the occurrence of transition with another polarization. Hence, at either ground state the transitions with σ- and π-polarization, but different intensites, are expected. The calculated values for the energy of Co^{2+} level agree well with experimental results (Table 3, footnote[a]).

When the symmetry of octahedral position is reduced to C_s (Co^{2+} in chrysoberyl), E levels are split and A″ will be the ground state (Fig. 4). The A″ → A′ transitions are allowed in Z polarization, while A″ → A″, in X and Y polarization. The spin-orbit interaction causes additional splitting of levels (Fig. 4). The $E'_{1/2} \rightarrow E'_{1/2}$ transitions in this case will be allowed in X, Y, and Z polarization, which was observed in the experiments (Table 3). The levels of $^{VI}Co^{2+}$ energy in chrysoberyl with optimal parameters ($Dq = 940$, $B = 860$, $C = 3700$, $v = 1650$, $v' = -610$, and $\alpha = 0$ cm^{-1}), calculated in the approximation of trigonal field, describe well the experimental spectrum.

The ground state of Co^{2+} in tetrahedral position is A, or A″ in the crystal field of symmetry D_2, or C_s, respectively (Fig. 5). In beryl, Co^{2+} replaces Be^{2+} (point symmetry of position D_2).Transition A → B_1, B_2, and B_3 are allowed in X, Y, and Z polarization, respectively (Table 2). Thus, the axis of the X spectrum coincides with the axis ***c*** || [0001] crystal and axis Z with [$2\bar{1}\bar{1}0$] || **a**. Spin-orbit interaction results in the fact that $E_{1/2} \rightarrow E_{1/2}$ are allowed in any polarization. Calculation of splitting of the levels caused by spin-orbit coupling, in approximation of cubic crystal field in first order, shows that the $^4T_2(F)$, $^4T_1(F)$ and $^4T_1(P)$ terms split into three levels each: $^4T_2(F) \rightarrow 5185$, 5410, 5545 cm^{-1}; $^4T_1(F) \rightarrow 8201$, 8578, 9207 cm^{-1}, and $^4T_1(P) \rightarrow 18052$, 18462, 18704 cm^{-1} (E⊥***c***). Experimental values of energy of levels (Table 4) at 80 K (E⊥***c***) are close enough to calculated values.

In chrysoberyl, the Co^{2+} ions, in addition to octahedral positions of Al^{3+}, can also occupy tetrahedral positions of Be^{2+} (point symmetry of position C_s). Transitions A″ → A′ are allowed in Z polarization, and A″ → A″ in X and Y polarizations. In this case consideration of spin-orbit interaction also removes the prohibition of the transitions $E'_{1/2} \rightarrow E'_{1/2}$ with any polarization (Fig. 5). However, as mentioned above, no bands of absorption from ions $^{IV}Co^{2+}$ in chrysoberyl were revealed, probably because of the low concentration of Co ions (Table 1).

The calculation of energy levels $^{IV}Co^{2+}$ in beryl is carried out in approximation of both cubic and trigonal crystal fields. The results of calculation of $^{IV}Co^{2+}$ energy levels in these approximations are shown in Table 4, footnote[a,b]. Calculation with application of $\alpha L(L + 1)$ does not reduce the deviation of calculated energy values from experimental ones in beryl.

As mentioned above, the absorption band in beryl in the region 12 500–8300 cm^{-1} with maxima at 11 600(π + σ) and 9900(σ)cm^{-1} is assigned to Co^{3+} replacing Al^{3+}. Polarization dependence of the spectrum can be explained by the following scheme. In the octahedral crystal field the term ^5D of Co^{3+} is split into

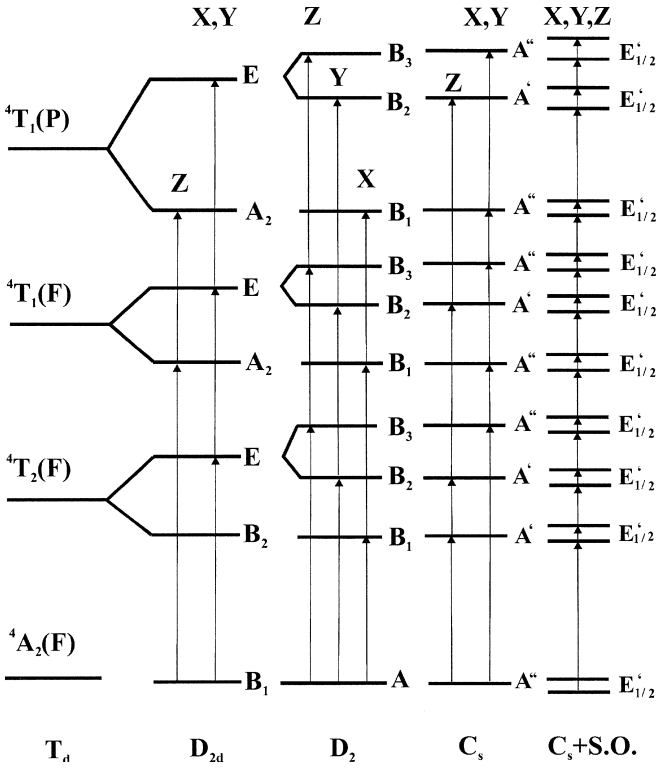

Fig. 5 Scheme of splitting of energy levels of Co^{2+} in tetrahedral sites at decreasing symmetry of environment $T_d \rightarrow D_{2d} \rightarrow D_2$ or $T_d \rightarrow D_{2d} \rightarrow C_s$

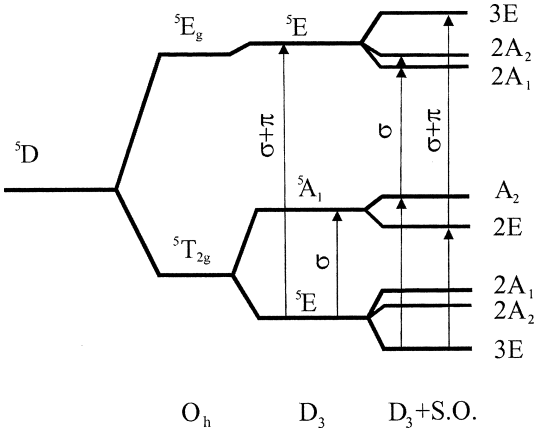

Fig. 6 Scheme of splitting of energy levels of Co^{3+} in octahedral sites at decreasing symmetry of environment $O_h \rightarrow D_{3d} \rightarrow D_3$

ground $^5T_{2g}$ and excited ^5E_g levels. The trigonal field splits $^5T_{2g}$ into ^5E and $^5A_1$ levels. Consideration of spin-orbit interaction removes the degeneration of E levels. Thus, according to the selection rules for D_3 symmetry (Table 2), $E \rightarrow E$ transitions are allowed in $\pi + \sigma$, whereas $E \rightarrow A_1$, A_2 in σ polarization (Fig. 6). Unfortunately, because of the overlap of absorption bands $^{VI}Co^{2+}$ (transitions $^4T_{1g} \rightarrow {}^4T_{2g}$) and $^{IV}Co^{2+}$ ($^4A_2 \rightarrow {}^4T_1$), it is imposible precisely to establish the position of absorption band maxima of Co^{3+}.

Our calculations of Co^{2+} spectra show that, in general, Trees' correction considerably improves the accuracy of calculations of the levels. This effect is particularly noticeable for $^4T_{1g}(P)$ and higher-energy levels. However, the optimal values α for the energy levels of different terms are different. Therefore, Table 3 gives the value α, which significantly improves the accuracy of calculations of main energy levels. Consideration of Trees' correction in calculations of the energy of $^{VI}Co^{2+}$ levels in chrysoberyl, however, did not significantly improve the accuracy of calculations of energy levels, most likely because the contributions from lower symmetry fields were neglected. This is also true for Co^{2+} in tetrahedral position.

Conclusions

Thus, the agreement of experimental and calculated locations of the Co^{2+} energy levels shows that the assignment of main absorption bands is reasonable. Polarization dependence of these bands can be explained only when the spin-orbit interaction is taken into account.

Our spectroscopic studies show evidence that Co ions enter beryl crystal structure in bi- and trivalent states, replacing octahedral site of Al^{3+} and tetrahedral site of Be^{2+} (Co^{2+}). It is shown that the uncontrolled impurity of ions $Cu^{2+} \rightarrow Be^{2+}$ in hydrothermal beryl is responsible for absorption with maxima close to 13 200(σ), 10 900(π), and 8500(σ) cm^{-1}. In chrysoberyl, Co^{2+} ions occupy Al^{3+} sites.

The data obtained indicate that the lacking charge of Co^{2+} in octahedral sites of beryl and chrysoberyl is compensated by the occurrence of Al^{3+} in Be^{2+} site. This is confirmed by the EPR observation of O^- centers as well as Al^{2+} in the Be^{2+} site after γ-irradiation of these crystals.

Acknowledgements The authors thank S.N. Lukin for recording EPR spectra at frequency of 74.5 GHz and V.D. Antsigin for recording optical absorption spectra.

References

Akridge JR, Kennedy JH (1979) Absorption and emission spectroscopy and magnetic susceptibility of sodium β-alumina doped with Mn, Co, and Ni. J Solid State Chem 29: 63–72

Alimpiev AI, Bukin GV, Matrosov VN, Pestryakov EV, Solntsev VP, Trunov VI, Tsvetkov EG, Chebotaev VP (1986) A tunable $BeAl_2O_4$: Ti^{3+} laser, in Russian, Kvantovaya Electronika, 14: 885–886

Barry WR, Troup GI (1969) EPR of Cr^{3+} ions in alexandrite. Phys Status Solidi 35: 811–814

Barry WR, Troup GI (1970) EPR of Fe^{3+} ions in chrysoberyl. Phys Status Solidi (b) 38: 229–234

Bukin GV, Volkov SYu, Matrosov VN, Sevastyanov BK, Timoshechkin MI (1978) Optical generation in alexandrite ($BeAl_2O_4 : Cr^{3+}$), in Russian, Kvantovaya Electronika 5: 1168–1169

Bukin GV, Matrosov VH, Orekhova VR, Remigailo YuL, Sevastyanov BK, Symonov EG, Solntsev VP, Tsvetkov EG (1981) Growth of alexandrite crystals and investigation of their properties. J Crystal Growth 52: 537–541

Edgar A, Hutton DR (1978) Exchange-coupled pairs of Cr^{3+} ions in emerald. J Phys (C): Solid State Phys 11: 5051–5063

Edgar A, Hutton DR (1982) Exchange-coupled pairs of Fe^{3+} ions in beryl. Solid State Commun 41: 195–198

Evdokimova OA, Belokoneva E.L, Artemenko VV, Dubovskaya VM, Urusov VS (1989) Location of impurity cations in synthetic cobalt- and copper-bearing beryls according to precise X-ray structural analysis, EPR and optical spectroscopy data, in Russian. Krstallografiya 34: 723–730

Farrell EF, Fang JH and Newnham RE (1963) Refinement of the chrysoberyl structure. Am Mineral 48: 804–810

Forbes CF (1983) Analysis of the spin-Hamiltonian parameters for Cr^{3+} in mirror and inversion sites of alehandrite ($Al_{2-x}Cr_{x}$-BeO_4). Determination of the relative site occupancy. J Chem Phys 79: 2590–2599

Herzberg G (1969) Electronic spectra and electronic structure of polyatomic molecules. Mir, Moscow, USSR, 772 p (translated from Herzberg G 1966. Molecular spectra and molecular structure. III. Electronic spectra and electronic structure of polyatomic molecules. Toronto)

Hofmann SK, Goslar J (1982) Crystal-field theory and EPR parameters in D_2 and C_{2v} distorted tetrahedral copper (II) complexes. J Solid State Chem 44: 343–353

Kharchenko EI, Solntsev VP (1981a) An exchange-coupled pairs of Cr^{3+} and Ti^{3+} ions in beryl, in Russian. In: Trudy Instituta Geologii i Geofiziki, Akademiya Nauk SSSR, issue 450. Novosibirsk, pp 60–68

Kharchenko EI, Solntsev VP (1981b) A theoretical-group and crystallographic analysis of possible pairs of impurity ions in crystals with beryl structure, in Russian. In: Trudy Instituta Geologii i Geofiziki, Akademiya Nauk SSSR, issue 487. Novosibirsk, pp 155–163

Khranenko GG, Solntsev VP (1988) Isomorphous substitutions in synthetic beryls, in Russian. In: Trudy Instituta Geologii i Geofiziki, Akademiya Nauk SSSR, 487. Novosibirsk, pp 94–99

Lebedev AS, Klyakhin VA, Solntsev VP (1988) Crystal chemistry features of hydrothermal beryls, in Russian. In: Trudy Instituta Geologii i Geofiziki, Akademiya Nauk SSSR, 708. Novosibirsk, pp 75–94

Maki AH, Edelstein N, Davison A, Holm RH (1964) EPR studies of electronic structure of bis(maleonitriledithiolato) copper (11), -nickel (111), -cobalt (11), -rhodium (11) complexes. J Am Chem Soc 86: 4580–4587

McClure DS (1962) Optical spectra of transition-metal ions in corundum. J Chem Phys 36: 2757–2779

McGarvey BR (1969) Charge transfer in the metal-ligand bond as determined by electron spin resonance. In: Teh Fu-Yen (ed) Electron spin resonance of metal complexes. Adam Hilger Ltd, London, pp 1–11

Morosin B (1972) Structure and thermal expansion of beryl. Acta Crystallogr (B) 28: 1899–1903

Pappalardo R, Wood DL, Linares RC (1961) Optical absorption study of Co-doped oxide system. J Chem Phys 35: 2041–2059

Rae AD (1969) Relation between the experimental Hamiltonian and the point symmetry of a paramagnetic species in a crystal. J Chem Phys 50 : 2672–2685

Ray DK (1961) Theory of covalent bond and the analysis of a spectrum paramagnetic resonance in corundum, in Russian. Sov Phys-Solid St 3: 2223–2239

Rodionov AYa, Solntsev VP, Weis NS (1987) Crystallization and properties of colouring varieties of gas-transport beryl, in Russian. In: Trudy Insituta Geologii i Geofiziki, Akademiya Nauk SSSR, 679 Novosibirsk, pp 41–53

Shand ML, Walling JC (1982) Excited-state absorption in the lasing wavelength region of alexandrite. IEEE J Quantum Electron QE-18: 1152–1155

Solntsev VP, Lebedev AS, Pavlyuchenko VS, Klyakhin VA (1976) Copper centers in synthetic beryl, in Russian. Sov Phys Solid State 46: 1396–1398

Solntsev VP (1981) The nature of colour centers and EPR in beryl and chrysoberyl, in Russian. In: Trudy Instituta Geologii i Geofiziki, Akademiya Nauk SSSR, 499. Novosibirsk, pp 92–140

Solntsev VP (1982) The colour centres and EPR in chrysoberyl with Mn and Ti impurities, in Russian. Zhurnal prikladnoi spektroskopii 37: 839–843

Solntsev VP, Khranenko GG (1989) The EPR of radiation defects in beryl. Sov Phys Solid State 31: 292–295

Sviridov DT, Smirnov Yu F (1977) The theory optical spectra of transition metal ions, in Russian. Nauka, Moscow, USSR, pp 328

Sviridov DT, Sviridova RK, Smirnov Yu F (1976) Optical spectra of transition metal ions in crystals, in Russian. Nauka, Moscow, USSR, pp 266

Taran MN, Rossman GR (2001) Optical spectra of Co^{2+} in three synthetic silicate minerals. Am Mineral 86: 889–895

Townsend MG (1964) Cobaltous ion in alumina. J Phys Chem 68:1569–1572

Trees RE (1951) Configuration interaction in Mn (II). Phys Rev 83: 756–760

Trees RE (1952) The L(L + 1) correction to the Slater formulas for the energy levels. Phys Rev 85: 382

Veremeichik TF, Grechushnikov BN, Kalinkina IN, Sviridov DT (1977) Trees correction for d^3-configuration in a strong field scheme. Configuration of the d^3-electron in trigonal field, in Russian. Zhurnal Prikladnoi Spektroskopii 26: 131–136

Walling JC, Peterson OG, Jenssen HP, Morris RC, O'Dell EW (1980) Tunable alexandrite lasers. IEEE J Quantum Electron QE-16: 1302–1314

Wildner M (1996) Polarized electronic absorption spectra of Co^{2+} ions in the kieserite-type compounds $CoSO_4 \cdot H_2O$ and $CoSeO_4 \cdot H_2O$. Phys Chem Miner 23: 489–496

Wildner M, Langer K (1994) Co^{2+} in trigonal fields of oxygen-based structures; electronic absorption spectra of $K_2Co(SeO_3)_2$, $K_2Co_2(SeO_3)_3$ and $K_2Co_2(SeO_3)_3 \cdot 2H_2O$. Phys Chem Miner 20: 460–468

Wood DL, Nassau K (1968) The characterization of beryl and emerald by visible and infrared absorption spectroscopy. Am Mineral 53: 777–800

Zverev GM, Prokhorov AM (1960) Electron paramagnetic resonance and spin-lattice relaxation of the Co^{2+} ion in corundum, in Russian. J Exp Theor Phys (USSR) 39: 57–63